Journal of Technomaterial Physics Vol. 4, No. 2, 2022 | 87-96

talenta PUBLISHER

JoTP
Journal of Technomaterial Physics

The Synthesis and Characterization of Iron Sand-Based $CuFe_2O_4$ as Heavy Metal Ion Adsorbent

Tika Mirdha Waty[1] and Sudiati[2*]

[1,2]Departement of Physics, Faculty of Mathematics and Natural Science, Universitas Sumatera Utara, Jalan Bioteknologi No.1 Kampus USU, Medan 20155, Indonesia

ABSTRACT This study aimed to synthesize iron sand-based Copper Ferrite ($CuFe_2O_4$) using the coprecipitation method. The iron sand was taken from South Cianjur and used as a Fe cation source to synthesize $CuFe_2O_4$ nanoparticles. Three composition variations of $CuCl_2.6H_2O$ and iron sand (Fe_3O_4) were employed, i.e., 1:1, 1:2, and 2:1. Samples were characterized using *X-Ray Diffraction* (XRD), *Scanning Electron Microscopy - Energy Dispersive X-Ray* (SEM-EDX), and *Atomic Adsorption Spectroscopy* (AAS). The XRD analysis exhibits three synthesis-phase results: $CuFe_2O_4$, Fe_2O_3, and CuO. The produced $CuFe_2O_4$ has two crystal structures: t-$CuFe_2O_4$ in 1:2 variation and c-$CuFe_2O_4$ in variations 1:1 and 2:1. Adding Cu resulted in smaller crystal size and higher lattice parameters. SEM-EDX analysis of 1:2 sample variation showed a round-shaped particle of 102.57 nm. AAS analysis showed that the increased mole of Cu decreases the heavy metal, including Pb and Mn, adsorption capacity. The largest adsorption capacity was found in the 1:2 (60.698 mg/g).

Keywords: Adsorbent, $CuFe_2O_4$, Nanoparticles, Iron Sand, Spinel Ferrite

Received 5 January 2022 | Revised [15 August 2022] | Accepted [29 August 2022]

1. Introduction

Technology development has resulted in various material-producing innovations, including magnetic nanoparticle materials. One of the magnetic nanoparticles that become the subject of continuous development is the spinel ferrite-based magnetic nanoparticle. [1]. The magnetic nanoparticle helps remove toxic metal ions from water through their magnetic properties, high chemical stability, facile synthesis, and good recyclability.

Heavy metal has caused serious environmental problems [2]. It harms human health when consumed in large amounts for a long time. Long-term consumption of Pb-polluted food can damage one's health and learning ability, hampering Hemoglobin synthesis and damaging bone marrow, liver and kidney functions, and nervous systems [3].

*Corresponding author at: Jalan Bioteknologi no.1 Medan, 20155, Indonesia

E-mail address: sudiati@usu.ac.id

Existing metal ion removal methods from water primarily include chemical, biological, and physical approaches. Common approaches to removing and recycling heavy metal ions from wastewater include chemical precipitation, coagulation, ion exchange, filtration, reverse osmosis, biological maintenance, and physical adsorption. The last-mentioned approach is one of the most efficient and economical methods [4].

In this study, iron sand-based $CuFe_2O_4$ was used to process waste through the adsorption method. Iron sand is known to contain magnetic minerals like magnetite (Fe_3O_4), hematite (α-Fe_2O_3), and maghemite (γ-Fe_2O_3), which can be applied to various fields [5] [6]. Spinel ferrite is represented as MFe_2O_4 (M = Ni, Mn, Co, and Cu), showing a unique catalytic efficiency in the oxidation method. Copper Ferrite ($CuFe_2O_4$) nanoparticle plays an important role in various heterogeneous catalytic purposes due to their simple isolation from treatment solution, high chemical stability, and decreased metal leaching [7].

2. EXPERIMENTAL

2.1 Material

Materials used in this study were natural iron sand is obtained from Southern Cianjur Coast (200 mesh), copper chloride ($CuCl_2.2H_2O$), 37% of hydrochloric acid (HCl), 2M of sodium hydroxide (NaOH), lead (II) nitrate ($Pb(NO_3)_2$), manganese chloride ($MnCl_2.6H_2O$), DI water and ethanol.

2.2 Synthesis of $CuFe_2O_4$ Nanoparticle

Iron sand-based-$CuFe_2O_4$ nanoparticle was synthesized using the coprecipitation method. $CuCl_2.2H_2O$ was dissolved with HCl 37%, while the iron sand was dissolved using DI water. The variations of $CuCl_2.2H_2O$: iron sand were 1:1 (0,017 mole: 0,017 moles), 1:2 (0,017 moles: 0,034 moles), and 2:1 (0,034 mole: 0,017 moles). NaOH 2M was added to the sample and stirred for 120 minutes at 500 rpm. After that, samples were deposited using a permanent magnet, separated from the contaminants, and washed using aqua dest and ethanol to reach pH 7. The deposits were dried out using an oven and calcining furnace, generating $CuFe_2O_4$ powder.

2.3 Characterization Test

XRF Test was performed to find the elements in the iron sand. Next, it was done to determine the crystal structure and size of the $CuFe_2O_4$ nanoparticle samples. Then, SEM-EDX was performed to see the particle size and the main constituents of $CuFe_2O_4$ nanoparticle. Lastly, AAS was performed to determine the heavy metal (Pb and Mn) ion adsorption capacity of the $CuFe_2O_4$ nanoparticle.

3. RESULT AND DISCUSSION

3.1 X-Ray Fluorescence (XRF) Test

Table 1 displays the elements of South Cianjur iron sand, following the XRF test result. It contained 22 elements, and Fe was the most dominant element (70.548 %). High Fe content asserts that iron sand has magnetic properties as a natural oxide [8].

Table 1. XRF Analysis on elements of South Cianjur iron sand

Element	Content Percentage (%)
Fe	70.548
Ti	10.537
Mg	6.985
Si	4.389
Al	2.727
17 other components	4.816

3.2 X-Ray Diffraction (XRD) Analysis

Figure 1 displays XRD characterization result Figure 1(a) shows that 1:1 and 2:1 $CuFe_2O_4$ variations exhibit a cubic crystal structure with the *space group* Fd3m, which is in line with ICDD 01-074-8585. The main peak at 35,5711^o - 35,5971^o is the field's peak (311). Other peaks in $CuFe_2O_4$ sample were at the field (220), (400), (422), (440), (531), and (622). This is in line with a previous study [9].

Meanwhile, the 1:2 variation has the same pattern as ICDD 00-034-0425. The XRD result shows the tetragonal crystal structure. The main peak at area 2 was around 35,8051˚, which was the field's peak (211). This is in line with [10] 1:2 stoichiometric comparison using the sol-gel method. Other peaks in $CuFe_2O_4$ sample were at (103), (112), (202), (220), (312), (106), (321), (224), and (400). Impurities, i.e., Fe_2O_3 and CuO, were present in the 1:1 and 2:1 sample variations, while in the 1:2 sample variation, only Fe_2O_3 was present.

Figure 1(b) exhibited the highest peak among the three samples. The highest 2θ peak position (311) for 1:1 and 2:1 variations exhibited a slight peak shift. The difference in 2θ peak and shift may be attributed to the samples' different Cu and Fe composition variations. Sample variation of 1:1 exhibits the highest intensity among other sample variations.

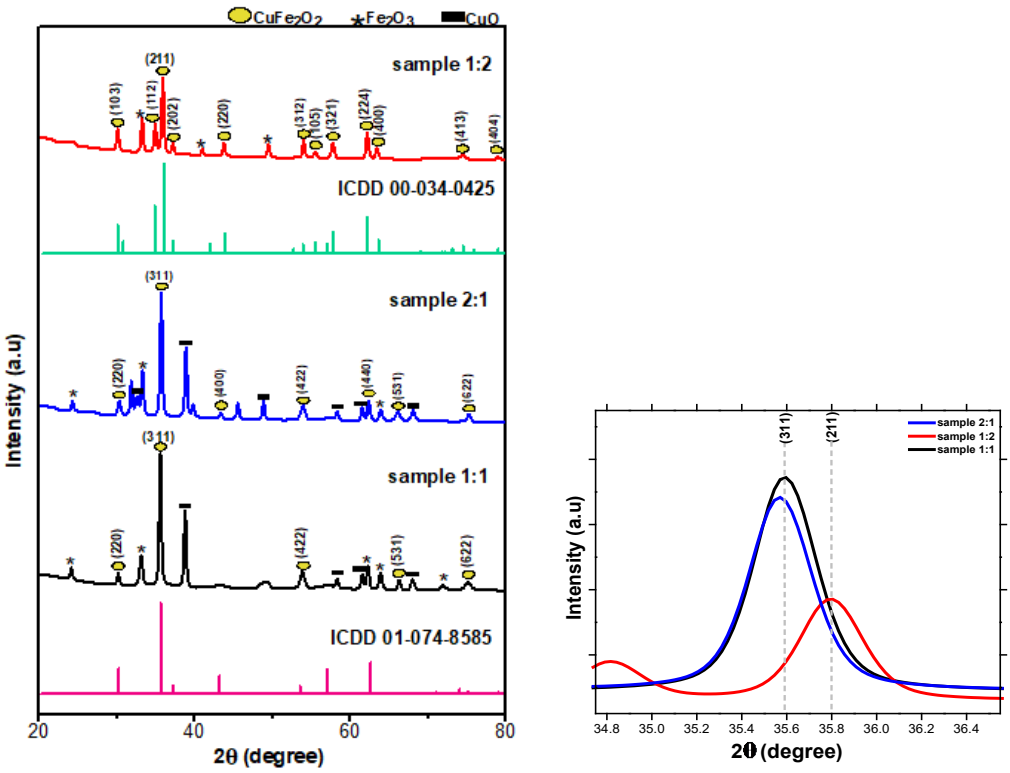

(a) (b)

Figure 1. (a) XRD pattern of $CuFe_2O_4$ nanoparticle (b) Magnified

The crystal size was calculated using the Scherrer formula, and the FWHM value of XRD data was presented in Table 2. The average crystal size of the $CuFe_2O_4$ nanoparticle with concentration variation of 1:1, 1:2, and 2:1 was 22.330 nm, 26.656 nm, and 22.133 nm, respectively. The crystal size of iron sand-based copper ferrite with coprecipitation ranges between 23 and 90 nm [11].

As shown in Figure 2, the sample variation of 2:1 has the smallest crystal size (22.33 nm), which may be attributed to the amount of atomic Cu in the sample. On the other hand, sample 1:2 has the largest crystal size (26.656 Å) among other sample variations due to the high amount of Fe.

Table 2. $CuFe_2O_4$ crystal size calculation result

Sample	2θ (deg)	FWHM (deg)	Crystal size (nm)
A (1:1)	30.1472	0.307	26.79925672
	35.5638	0.307	27.1754449
	53.8748	0.614	14.51323866
	66.3388	0.307	30.91447093
	75.2088	0.8187	12.24819105
		Mean	**22.33012045**
B (1:2)	29.951	0.307	26.78694367
	34.7884	0.307	27.1172171
	35.769	0.307	27.1911046
	37.0813	0.307	27.29375531
	43.686	0.307	27.8786595
	53.9927	0.307	29.04167628
	55.478	0.4093	21.92967671
	57.7684	0.4093	22.16708806
	62.2287	0.307	30.22546866
	63.465	0.307	30.42536175
	74.5379	0.614	16.25854834
	79.0909	0.307	33.55790359
		Mean	**26.65611696**
C (2:1)	30.1075	0.4093	20.09920523
	35.542	0.307	27.17378743
	43.256	0.307	27.83698475
	53.8705	0.614	14.51296193
	62.397	0.307	30.25231921
	66.1195	0.614	15.43795294
	75.343	0.5117	19.61433301
		Mean	**22.13250636**

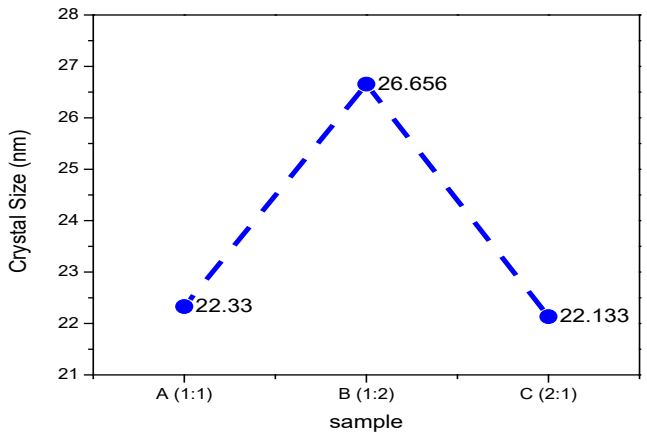

Figure 2. Graph of $CuFe_2O_4$ crystal size

Lattice parameter calculation using the Cohen method is presented in Table 3. Following the XRD data, $CuFe_2O_4$ nanoparticle with 1:1, 1:2, and 2:1 variation composition has a lattice parameter value of 8.355 Å, 6.796 Å, and 8.368 Å, respectively. In [11] study, the lattice parameter value of coprecipitated iron sand-based Copper Ferrite was 8.37 Å.

As shown in Figure 3, sample 1:2 exhibited the lowest lattice parameter (6.796 Å) among other variations, which may be attributed to the high amount of atomic FE. Sample 2:1 has the highest

lattice parameter value (8.368 Å) among other sample variations due to the high amount of atomic Cu.

Table 3 $CuFe_2O_4$ lattice parameter calculation result

Sample	hkl	2θ (Deg)	Lattice Parameter (Å)
A (1:1)	220	30.1472	8.377838081
	311	35.5638	8.365559995
	422	53.8748	8.330120266
	531	66.3388	8.329411205
	622	75.2088	8.373552711
		Mean	**8.355296451**
B (1:2)	112	29.951	7.301850771
	103	34.7884	8.148351872
	211	35.769	6.144080152
	202	37.0813	6.851862695
	220	43.686	5.855804871
	312	53.9927	6.34938196
	105	55.478	8.438758722
	321	57.7684	5.966779245
	224	62.2287	7.30275799
	400	63.465	5.858305064
	413	74.5379	6.486215624
	404	79.0909	6.843949262
		Mean	**6.795674852**
C (2:1)	220	30.1075	8.38862929
	311	35.542	8.370525331
	400	43.256	8.35967588
	422	53.8705	8.330735459
	440	62.397	8.41203861
	531	66.1195	8.353886112
	622	75.343	8.360845919
		Mean	**8.368048086**

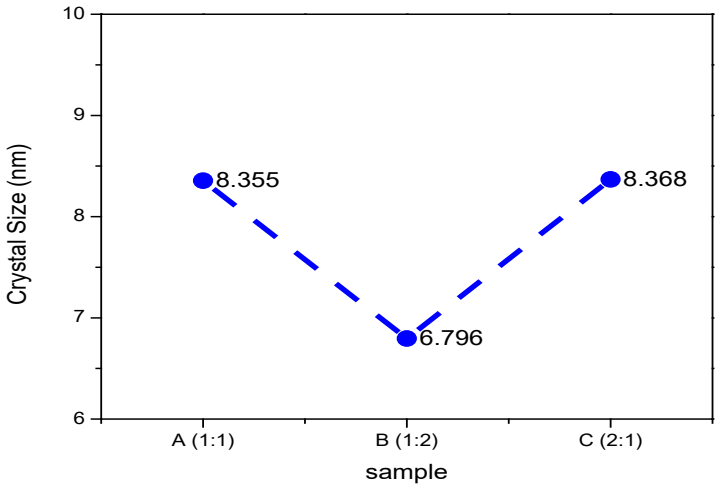

Figure 3. Graph of $CuFe_2O_4$ lattice parameter

3.3 Scanning Electron Microscope-Energy Dispersive X-Ray (SEM-EDX) Analysis

Figure 4 displays SEM-EDX characterization results. As shown in Figure 4, $CuFe_2O_4$ nanoparticle forms resemble sand grains, consistent with the previous study [12]. Sample 2:1 exhibited agglomeration that caused difficulty in measuring the grain size.

Figure 5 displays the histogram of $CuFe_2O_4$ nanoparticles. Figure 5 shows a sharp and wide increase with an average grain size of 102.57 nm. Thi et al. report that the average grain size of Copper Ferrite was 80-200 nm [13]. In this study, the calculation result shows that each grain of $CuFe_2O_4$ nanoparticle contains about four crystals (XRD results) with a crystal size of sample variation 2:1 was 22.133 nm.

Figure 6 displays the mapping result of $CuFe_2O_4$ nanoparticle. $CuFe_2O_4$ nanoparticle's constituents were Cu, Fe, and O, with a composition of 17.63%; 66.10%; and 16.27%, respectively. In other words, the sample contains only Cu, Fe, and O. The presence of Cu shows that Cu can bind Fe and O.

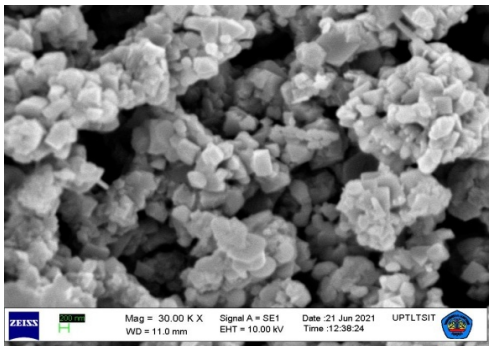

Figure 4. Morphology of 2:1 $CuFe_2O_4$ variation (30,000 of magnification)

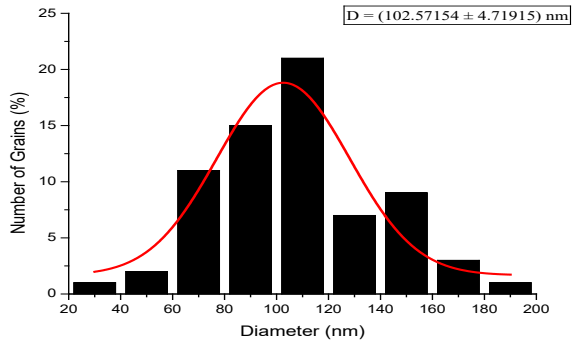

Figure 5. Histogram of 2:1 $CuFe_2O_4$ variation (Sample C)

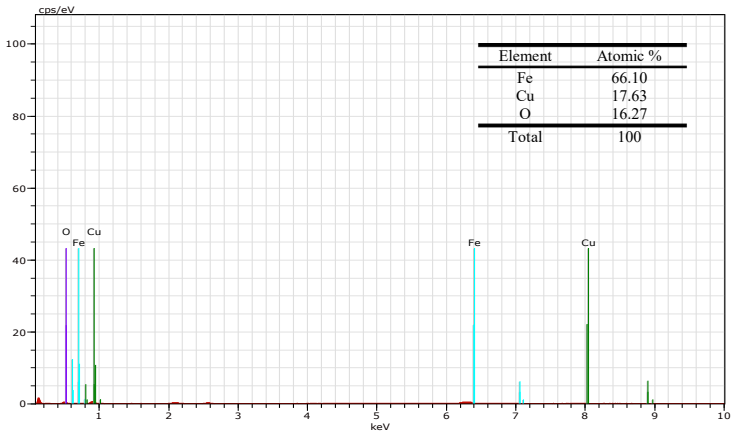

Figure 6. Spectrum mapping of $CuFe_2O_4$ of 2:1 variation (sample C)

3.4 Atomic Adsorption Spectroscopy (AAS) Analysis

The AAS test result is presented in Table 4. The sample with 1:2 concentration variation adsorbs lead Lead with a removal efficiency of 31.718% and an adsorption capacity of 60.632 mg/g. Taleb et al. found that the adsorption capacity of $CuFe_2O_4$ on Pb was 17.83 mg/g with pH 4.5, a temperature of 289 K, and an adsorbent weight of 0.02 grams [14].

As shown in Table 5, the sample with a 2:1 concentration variation exhibited the highest ability in adsorbing Mn, indicated by a removal efficiency of 0.6637% and an adsorption capacity of 0.196 mg/g. Tu et al. report that $SiO/CuFe_2O_4$/PANI composite adsorbent has an Mn adsorption capacity of 454.55 mg/g [15].

Table 4. Removal Efficiency and Pb adsorption capacity of $CuFe_2O_4$ nanoparticles

Sample (0.05 g)	Pb ion concentration (mg/L)		Absorbed Pb ion concentration (mg/L)	Pb removal efficiency (%)	Pb ion adsorption capacity (mg/g)
	Before adsorption	After adsorption			
A (1:1)	477.8947	428.631	49.2637	10.3083	19.70548
B (1:2)	477.8947	326.3158	151.5789	31.7180	60.63156
C (2:1)	477.8947	406.8947	71	14.8568	28.4

Table 5. Mn ion removal efficiency and adsorption capacity of $CuFe_2O_4$ nanoparticles

Sample (0.05 g)	Mn ion concentration (mg/L)		Absorbed Mn ion concentration (mg/L)	Mn removal efficiency (%)	Mn ion adsorption capacity (mg/g)
	Before adsorption	After adsorption			
A (1:1)	73.7615	73.4101	0.315	0.4754	0.14056
B (1:2)	73.7615	73.5945	0.167	0.2264	0.0668
C (2:1)	73.7615	73.2719	0.4896	0.6637	0.19584

As shown in Figure 7, the concentration variation of 1:2 is the best concentration to adsorb Pb and Mn with an adsorption capacity per adsorbent weight of 60.698 mg/g, which may be attributed to the high Fe moles.

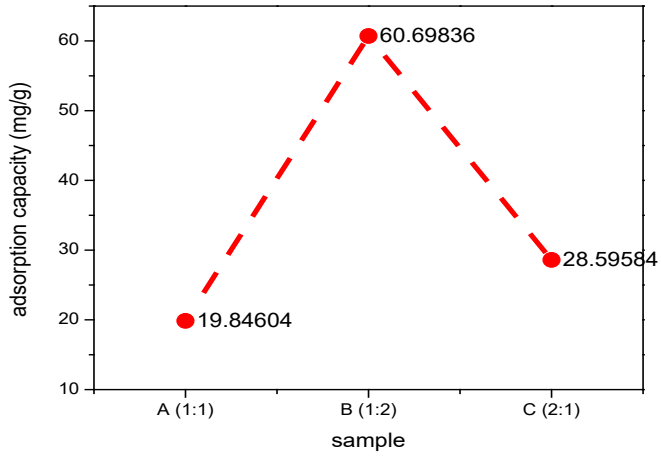

Figure 7. Pb and Mn ion adsorption capacity of $CuFe_2O_4$ nanoparticle

4. CONCLUSION

This study synthesized $CuFe_2O_4$ nanoparticles from iron sand in Cianjur Coast with mole variations of 1:1, 1:2, and 2:1. The result of XRD analysis shows that the crystal size decreases as atomic Cu increases and atomic Fe decreases. The SEM-EDX analysis result shows that the concentration variation of 2:1 has an average particle size of 102.57 nm with a sand grain shape. AAS analysis shows that Fe increase leads to higher Pb and Mn ion adsorption capacity. The highest adsorption capacity was found in the concentration variation of 1:2.

REFERENCES

[1] T. R. Simbolon, T. Sembiring, H. M. Hamid, D. A. Hutajulu, M. Rianna, A. M. S. Sebayang, A. P. Tetuko, E. A. Setiadi, M. Ginting, P. Sebayang, "Preparasi dan Karakterisasi Mikrostruktur dan Sifat Magnet $ZnFe_2O_4$. *J. Aceh Phys. Society,* vol. 10, no. 2, 2021.

[2] D. Sartika, E. Malis, and E. S. Mangunang, "Analisis Distribusi Nanopartikel Fe_3O_4 Terhadap Penyerapan Logam Berat Pb," *Jurnal Teknologi Technoscientia*, vol. 12, no. 1, 2019.

[3] K.T. Osman, "Soil pollution". In *Soil degradation, conservation and remediation*, pp. 149-226. Springer, Dordrecht, 2014.

[4] M. Hasanpour and M. Hatami, "Application of Three Dimensional Porous Aerogels as Adsorbent for Removal of Heavy Metal Ions From Water/Wastewater: A Review Study, *Advances in Colloid and Interface Science*, vol. 284, no. 102247, 2020.

[5] E. Widianto, Kardiman, and N. Fauji, "Karakterisasi Pasir Besi Alam Pantai Samudera Baru dan Pemanfaatannya sebagai Filler pada Sistem Penyaring Elektromagnetik," *Jurnal Riset Sains dan Teknologi*, vol. 2, no. 1, 2018.

[6] D. L. Puspitarum, G. Safitri, H. Ardiyanti, and M. S. Anrokhi, "Karakterisasi dan Sifat Kemagnetan Pasir Besi di Wilayah Lampung Tengah," *Jurnal Pendidikan Fisika FKIP UM Metro, vol.* 7, no. 2, 2019.

[7] M. Zangiabadi, A. Saljooqi, T. Shamspur, and A. Mostafavi, "Evaluation of GO nanosheets decorated by CuFe2O4 and CdS nanoparticles as photocatalyst for the degradation of dinoseb and imidacloprid pesticides", *Ceramics International*, vol. *46*, no. 5, pp. 6124-6128, 2020.

[8] A. T. Mubarok, "Variasi Suhu Annealing pada Sintesis $CoFe_2O_4$ dari Pasir Besi Sungai Bengawan Solo," Undergraduate Thesis, Universitas Sebelas Maret, Surakarta, 2019.

[9] A. Subha, M. G. Shalini, and C. Sahoo, "Magnetic Studies of $CuFe_2O_4$ Nanoparticles Prepared by Co-Precipitatation Method," *AIP Conference Proceedings*, vol. 1728, no. 020416, 2016.

[10] M. Choupani and A. Gholizadeh, "The Effect of Calcination Temperature on the X-Ray Peak Broadening of t-$CuFe_2O_4$," *Progress in Physics of Applied Materials,* vol. 1, no. 1, 2021.

[11] F. M. A. Saputra, A. Yulianto, and M. P. Aji, "Sintesis Pigmen Magnetik *Copper Ferrite* ($CuFe_2O_4$) Berbahan Dasar Pasir Besi Menggunakan Metode Kopresipitasi," *Unnes Physics Journal.* vol. 5, no. 2, 2016.

[12] R. M. Ali, M. R. Elkatory, H. A. Hamad, "Higly Active and Stable Magnetically Recyable $CuFe_2O_4$ as a Heterogenous Catalyst for Efficient Conversion of Waste Frying Oil to Biodiesel. *Fuel,* vol. 268, no. 117297, 2020.

[13] T. U. T. Thi, V. H. Phan, H. T. P. Nguyen, T. L. Nguyen, A. N. Vu, and T. K. Le, "Synthesis of Magnetic $CuFe_2O_4/Fe_2O_3$ Core-Shell Materials and Their Application in Photo-Feton Like Process with Oxalic Acid as a Radical-Producing Source, *Journal of*

Asian Ceramic Societies, vol. 9, no. 3, 2021.

[14] M. A. Taleb, R. Kumar, A. A. Al-Rashdi, M. K. Seliem, M. A. Barakat, "Fabrication of SiO2/$CuFe_2O_4$/Polyaniline Composite: a Highly Efficient Adsorbent for Heavy Metals Removal from Aquatic Environment," *Arabian Journal of Chemistry,* vol. 13, no. 10, 2020.

[15] Y-J. Tu, C-F. You, M-H. Chen, and Y-P. Duan, "Efficient Removal/Recovery of Pb Onto Environmentally Friendly Fabricated Copper Ferrite Nanoparticles," *Journal of The Taiwan Institute of Chemical Engineers*, vol. 71, 2017.